REPORT DOCUMENTATION PAGE	Form Approved OMB No. 0704-0188

1. AGENCY USE ONLY (Leave blank)	2. REPORT DATE 18.Apr.06	3. REPORT TYPE AND DATES COVERED MAJOR REPORT

4. TITLE AND SUBTITLE
COMBINED SINGULARITY AVOIDANCE FOR VARIABLE-SPEED CONTROL MOMENT GYROSCOPE CLUSTERS.

5. FUNDING NUMBERS

6. AUTHOR(S)
MAJ RICHIE DAVID J

7. PERFORMING ORGANIZATION NAME(S) AND ADDRESS(ES)
UNIVERSITY OF SURREY

8. PERFORMING ORGANIZATION REPORT NUMBER

CI04-1769

9. SPONSORING/MONITORING AGENCY NAME(S) AND ADDRESS(ES)
THE DEPARTMENT OF THE AIR FORCE
AFIT/CIA, BLDG 125
2950 P STREET
WPAFB OH 45433

10. SPONSORING/MONITORING AGENCY REPORT NUMBER

11. SUPPLEMENTARY NOTES

12a. DISTRIBUTION AVAILABILITY STATEMENT
Unlimited distribution
In Accordance With AFI 35-205/AFIT Sup 1

12b. DISTRIBUTION CODE

13. ABSTRACT (Maximum 200 words)

14. SUBJECT TERMS

15. NUMBER OF PAGES
15

16. PRICE CODE

17. SECURITY CLASSIFICATION OF REPORT	18. SECURITY CLASSIFICATION OF THIS PAGE	19. SECURITY CLASSIFICATION OF ABSTRACT	20. LIMITATION OF ABSTRACT

Combined Singularity Avoidance for Variable Speed Control Moment Gyroscope Clusters

Vaios J. Lappas*, Sajjad Asghar†, David J. Richie ‡, and Phil L. Palmer§

University of Surrey , Guildford, UK, GU2 7XH

D Fertin¶ *European Space Agency*

ESTEC, Nordwijk, Netherlands

||

Introduction

Variable Speed Control Moment Gyroscopes (VSCMGs), defined by Schaub in [1], effectively applied to combined energy storage and attitude control in [2, 3], and further studied by Yoon and Tsiotras in [4, 5], can avoid attitude singularities by varying wheel speed. However, this device's key advantage lies in torque amplification via gimballing (i.e. operating in its CMG mode). The primary limitation of this CMG mode, though, is the existence of gimbal-lock singularity states. Avoiding escapable singularity states, studied extensively by Wie for CMGs [6] and Schaub for VSCMGs [7], is exacerbated in the case of simultaneous attitude and power tracking requirements [5]. Although [5] gives an algorithm for combined energy storage and attitude control with VSCMG singularity avoidance, it does not directly evaluate this algorithm with respect to other robust CMG singularity avoidance methods from the literature. For this reason, two practical steering laws were adapted from previous results for this challenging case and compared to the results given in [5]. First, Wie's Generalized Singularity Robust (GSR) steering law, originally developed

*Lecturer, Surrey Space Centre, School of Electronics and Physical Sciences, University of Surrey. Email: v.lappas@surrey.ac.uk. Member AIAA.

†PhD Student, Department of Mathematics, University of Surrey. Email: s.asghar@surrey.ac.uk.

‡Graduate Student, Surrey Space Centre, School of Electronics and Physical Sciences, University of Surrey. Email: d.richie@surrey.ac.uk. Senior member AIAA.

§Reader, Surrey Space Centre, School of Electronics and Physical Sciences, University of Surrey. Email: p.palmer@surrey.ac.uk. Member AIAA.

¶Control Systems Engineer, Email: XXXXX@YYYY.ZZZ

||The views expressed in this article are those of the authors and do not reflect the official policy or position of the United States Air Force, Department of Defense, or the U.S. Government

for attitude tracking with CMGs [8] was modified to use VSCMGs. Although the GSR effectively perturbs gimbals through locked configurations when compared to classical CMG methods (see [6, 9, 10]), it also imparts small attitude torque errors which can linger for a few minutes after a CMG singularity. This problem can be disruptive to some space missions that use satellite off-pointing (e.g. precision earth imaging) where accurate trajectory tracking during operations is paramount. However, VSCMG wheel speed freedom permits the modified GSR to remove these errors, but is limited in the power tracking case. Further extending this modified GSR to track power in the null subspace of the VSCMG steering dynamics (as in [2, 3]) enables an improved steering law that overcomes CMG singularity, eliminates small attitude errors, and tracks a desired flywheel energy storage/drain profile. Second, Schaub's VSCMG with null motion algorithm [7], designed to exploit its CMG mode while more efficiently accommodating gimbal-lock singularity than previous VSCMG approaches, was modified for the power tracking case. As demonstrated here, the adapted GSR and the modified VSCMG plus null motion algorithms perform comparably (showing a small improvement) over Yoon/Tsiotras' results from [5].

Simultaneous Attitude and Power Tracking Model

As shown in [3], a model encompassing the spacecraft dynamics, kinematics, required attitude reference torque, and VSCMG attitude plus power steering is

$$\overline{N_d} = I_{sc}\dot{\omega} + \tilde{\omega}I_{sc}\omega + B\ddot{\delta} + E\dot{\Omega} + D\dot{\delta} + F\Omega \tag{1}$$

$$\dot{\beta} = \frac{1}{2}q(\beta)\omega \tag{2}$$

$$\overline{N_r} = kI_{sc}q^T(\beta)\beta_r + KI_{sc}(\omega - \omega_r) - \tilde{\omega}I_{sc}\omega \tag{3}$$

$$q(\beta) = \begin{bmatrix} -\beta_1 & -\beta_2 & -\beta_3 \\ \beta_0 & -\beta_3 & \beta_2 \\ \beta_3 & \beta_0 & -\beta_1 \\ -\beta_2 & \beta_1 & \beta_0 \end{bmatrix} \tag{4}$$

$$B\ddot{\delta} + E\dot{\Omega} + D\dot{\delta} + F\Omega = \overline{N_r} + \overline{N_d} \tag{5}$$

$$\Omega^T I_{ws_d}\dot{\Omega} = V\dot{\Omega} = P_r \tag{6}$$

where $\overline{N_d}$ is the inertial torque acting on the combined system of the spacecraft platform plus the VSCMGs, I_{sc} is the system inertia assuming the gimballed VSCMG inertia (from rotor dynamics) is negligible, β is the Euler parameter set $(\beta_0, \beta_1, \beta_2, \beta_3)$ representing the satellite body frame orientation with respect to the inertial frame, ω is the angular velocity of the body frame with respect to the inertial frame expressed in body frame coordinates, $\dot{\beta}$ and $\dot{\omega}$ are the body frame time derivatives of β and ω, β_r, and ω_r are command reference versions of β and ω, δ is an $n \times 1$

column matrix of n-VSCMG gimbal angles, $\dot{\delta}$ and $\ddot{\delta}$ are $n \times 1$ gimbal angular velocity and angular acceleration column matrices, $\tilde{\omega}$ is a 3×3 skew-symmetric matrix using the elements of ω; B, D, E, F are $3 \times n$ matrices transforming actuator parameters from the gimbal coordinate frame to the body frame where B is a function of δ and is constant in the body frame, D depends on ω, δ, and Ω, varies in the body frame, and is approximated as its wheel angular momenta component, E transfers the wheel acceleration to the body frame and is dependent upon the gimbal angles, and F depends on the gimbal angles and body angular velocity ω and is equivalent to the $\tilde{\omega}h$ defined in [5,6]. I_{ws_d} is a $n \times n$ diagonal matrix of VSCMG wheel spin-axis inertias. P_r is the required power to store/drain in the wheels, while P_w is the actual power contained in the wheels. Since $V = \Omega^T I_{ws_d}$, then $P_w = V\dot{\Omega}$. Finally, k is a positive gain scalar, K is a 3×3 positive definite gain matrix, and $\overline{N}_r$, which uses k and K, is the required torque for stable spacecraft attitude tracking.

Noted often in the literature (e.g. [1,3]), CMGs typically exploit torque amplification properties through gimbal rate control (i.e keeping gimbal motor torques small such that $\ddot{\delta} \approx 0$). The result is a velocity-based steering law to replace eq. 5 (assuming no external torques are applied)

$$E\dot{\Omega} + D\dot{\delta} = \overline{N}_r - F\Omega \tag{7}$$

This velocity-based steering law permits different combinations of gimbal rate and wheel acceleration (similarly torque) to achieve a desired attitude maneuver. One can store (drain) energy by increasing (decreasing) the wheel speeds in combinations that still permit the desired net torque for attitude tracking. Eq. 6 captures the goal for this additional requirement: get the actual power in the wheels, $P_w = V\dot{\Omega}$ to match a time-varying power profile, i.e. $P_w = P_r(t)$. From eqs. 6 and 7, one can define the set

$$\begin{bmatrix} E & D \\ V & 0_N \end{bmatrix} u = \begin{bmatrix} Q \\ S \end{bmatrix} u = \begin{bmatrix} N_c \\ P_c \end{bmatrix} \tag{8}$$

where $u = \left[\dot{\Omega}^T \dot{\delta}^T \right]^T$, $N_c = \overline{N}_r - F\Omega$, $P_c = P_r(t)$, $Q = [E \ D]$, 0_{1XN} is a $1 \times n$ matrix of zeros, and $S = [V \ 0_{1XN}]$. Eq. 8 enables simultaneously tracking a stable attitude reference and a power profile.

Attitude Singularity Avoidance

The fundamental VSCMG attitude steering problem is ensuring

$$Qu_c = Q \begin{bmatrix} \dot{\Omega} \\ \dot{\delta} \end{bmatrix}_c = N_c \tag{9}$$

which yields a general VSCMG steering law

$$\begin{bmatrix} \dot{\Omega} \\ \dot{\delta} \end{bmatrix}_c = Q^\dagger N_c \tag{10}$$

where $Q^\dagger$ is some generalized inverse of Q such as

$$Q^{\S\S} = W_1 Q^T \left(Q W_1 Q^T \right)^{-1} \tag{11}$$

In eq. 11, a weighting scheme is used to weight the gimbal and wheel command modes, thereby permitting a method for the wheels to take control near gimbal singularity and gimbal torque advantages to prevail everywhere else. One way to combat this is to use the Generalized Singularity Robust (GSR) steering law introduced by Wie et. al. in [8, 11]

$$\begin{bmatrix} \dot{\Omega} \\ \dot{\delta} \end{bmatrix}_c = Q^\star N_c \tag{12}$$

where

$$Q^\star = W_1 Q^T \left(Q W_1 Q^T + G \right)^{-1} \tag{13}$$

This method is adept at rescuing the system from gimbal lock, but does impart residual attitude torque error during the maneuver and for some time afterward. These errors can disrupt the ability to track a desired attitude during precision imaging operations. One solution is to use wheel control to eliminate these errors. This is done as follows. Let u_{true} be the commanded u required to achieve N_c, u_{GSR} be the u associated with the GSR, and u_{error} be the commands necessary to eliminate the tracking error caused by the GSR. Then the following equations apply

$$u_{true} = u_{GSR} + u_{error} \tag{14}$$

$$u_{GSR} = Q^\star N_c \tag{15}$$

$$Q u_{error} = N_{c_{error}} \tag{16}$$

$$u_{error} = Q^\ddagger N_{c_{error}} \tag{17}$$

Define $Q^\ddagger = W_2 Q^T \left(Q W_2 Q^T \right)^{-1}$, where the weighting matrix W_2 permits weighting between the wheels and gimbals independent of the weights in W_1 and only acts during singularity. Next, derive the error torque, $N_{c_{error}}$, where I_3 is the 3×3 identity matrix, as

$$N_{c_{error}} = N_{c_{true}} - N_{c_{GSR}} = N_c - Q Q^\star N_c = (I_3 - Q Q^\star) N_c \tag{18}$$

Finally, assemble the components of u_{true}, which now becomes the GSR correction steering law, $u_{GSRcorr}$ for VSCMGs

$$u_{GSRcorr} = u_{true} = Q^\star N_c + Q^\ddagger (I_3 - QQ^\star) N_c = Q^\diamond N_c \qquad (19)$$

Thus, $Q^\diamond = Q^\star + Q^\ddagger (I_3 - QQ^\star)$. Clearly, a logical choice for W_2 (where I_N is the $n \times n$ identity matrix) is

$$W_2 = \begin{bmatrix} I_N & 0_N \\ 0_N & W_2^\Upsilon I_N \end{bmatrix} \qquad (20)$$

where $W_2^\Upsilon = W_{2_0} e^{-\mu_2 \det\left(\frac{EE^T}{I_{ws_d} I_{ws_d}}\right)}$. It permits de-weighting the gimbal mode when constructing the attitude error correction torque (the gimbals are in singularity when W_2 acts). This thereby promotes the wheel mode as desired. In contrast, the choice for W_1 comes from typical applications such as found in [5]

$$W_1 = \begin{bmatrix} I_N & 0_N \\ 0_N & W_g \end{bmatrix} \qquad (21)$$

where $W_g = W_{g_0} e^{-\mu \kappa(D)}$. Although this W_1 matrix will work in theory, it is not practically efficient at keeping wheel and gimbal accelerations small during singularity avoidance.

Singularity Avoidance with Power Tracking

The technique to project power in the nullspace of the dynamics matrix (Q in this case) was shown in [3]. The steps are given in the Appendix. This yields the extended GSR simultaneous attitude and power tracking steering law, u_{new},

$$u_{new} = u_{GSRcorr} + u_n = Q^\diamond N_c + P_n S^T \left(SP_n S^T\right)^{-1} \left(P_c - SQ^\diamond N_c\right) \qquad (22)$$

3.0 Numerical Example

The utility of the extended GSR (eq. 22) and the modified VSCMG with null motion algorithms for attitude and power tracking are best viewed in the context of a practical example such as that from [5]. In this scenario, attitude and power tracking for five cases are investigated, I: no singularity robust steering, II: GSR steering with no attitude error correction, III: extended GSR with attitude error correction, IV: modified VSCMG+null motion from [7], and V: VSCMG attitude

and power tracking from [5]. The parameters used for these cases are listed in Table 1 while Table 2 highlights some performance results. More specifically, it compares attitude error, momentum wheel mode torque generated by each VSCMG ($N_{s_{max}}$), top wheel speed (in RPM), nominal wheel speed, and the percentage difference between the maximum and nominal wheel speeds. These are maximum values of respective physical quantities during the maneuver. However, attitude errors are compared only during the tracking phase and the initial transient phase is ignored. One can see the attitude error is increased in case II which is then corrected in cases III, IV, and V. In the overall scenario, smaller values of torque are required for cases II through V as compared to case I as well as smaller variation in wheel speed for the same cases. These results illustrate the improved efficiency of the proposed singularity avoidance plus attitude/power tracking methods (cases III, IV, and V).

The ensuing figures show the dynamic results of these tests. Vehicle attitude and power tracking results are shown in figure 1 (where 1(a) shows the reference and attitude tracking performance of cases I, III, IV, and V, all of which are similar, 1(b) shows the attitude tracking performance of case II, capturing its 4-channel quaternion tracking error in the 4 circles on the plot, and 1(c) shows the reference power and attitude tracking case applicable to all 5 cases) along with the CMG singularity condition for all 5 cases 1(d). It's important to note that all 5 cases have the same reference and actual power profile plots. This means that the cluster's unsaturated wheels perfectly track the given open-loop power profile. This follows directly from the cluster's VSCMG redundancy. Also, the tracking error from case II lasts more than 200 s. Unchecked, this tracking error can negatively impact precise imaging operations.

These VSCMG algorithms can be further investigated at the actuator level by examining figure 2. This figure shows the gimbal angle and wheel speed responses of the 5 cases. As is seen in these plots, the gimbal and wheel responses for cases III, IV, and V (relating to figures 2(c),2(d),2(e),and 2(f)) are quite difficult to delineate. However, cases I and II, reflected in figure 2(a) for the gimbal angles and 2(b) for the wheel speeds, show differences in actuator response after the key singularity (occurs just before 4000 s). In case I, which uses no singularity avoidance algorithm, the gimbal angles become fixed at a singularity and do not change for the remainder of the maneuver. Conversely, the wheel speeds increase motion at this singularity to account for this locked configuration. The result is that the VSCMGs become simple Momentum Wheels for the remainder of the maneuver. This result is also undesirable since the wheels cross zero and begin to spin in the opposite sense. In contrast, case II shows that the GSR is effective at keeping the actuators away from gimbal lock with the added performance degradation of the aforementioned attitude error.

4.0 Conclusions

The proposed extended GSR and modified Schaub with null motion algorithms eliminate small attitude errors for all time such that any escapable singularities occurring during a maneuver can be mitigated. In addition to this, a given power profile is simultaneously tracked completely in this case due to cluster redundancy based on employment of the power projection method from [3]. Both methods have a small performance improvement over Yoon/Tsiotras' complex gradient method in exploiting each VSCMG in the cluster's CMG-mode, avoiding CMG singularities, following a desired 3-axis attitude trajectory, and tracking a given flywheel battery power profile. This result forms a link between classical single-gimbal CMG and modern VSCMG theory. From it, one can see the relationship between the extended GSR, modified Schaub VSCMG+null motion steering law, and the Yoon/Tsiotras results from [5], each originally developed for a different purpose. Satellite designers can use this result to strike harmony between gimbal and wheel motion with important practical implications – the ability to maintain precise pointing during agile slewing operations while using VSCMG flywheels to store (drain) energy.

Appendix A: Projected Power in Null Space of Q

Define $u_n = \begin{bmatrix} \dot{\Omega} \\ \dot{\delta} \end{bmatrix}_{null}$ and the operator, P_n, which projects a vector, v onto the nullspace of Q. Then, one can use the step-by-step equation set below to derive the simultaneous wheel and gimbal steering law, u. Notice that in this equation set, $Q^\dagger$ represents any suitable generalized inverse, including $Q^\star$ or Q°.

$$Qu = N_c \tag{23}$$

$$Qu_n = 0 \tag{24}$$

$$u_n = P_n v \tag{25}$$

$$P_n = P_n P_n^T = I_n - Q^\dagger Q \tag{26}$$

$$u = Q^\dagger N_c + u_n \tag{27}$$

$$Su = S(Q^\dagger N_c + u_n) = P_c \tag{28}$$

$$Su_n = SP_n v = P_c - SQ^\dagger N_c \tag{29}$$

$$(SP_n)v = P_c - SQ^\dagger N_c \tag{30}$$

$$v = (SP_n)^\dagger (P_c - SQ^\dagger N_c) \tag{31}$$

$$v = P_n^T S^T \left(SP_n P_n^T S^T\right)^{-1} (P_c - SQ^\dagger N_c) \tag{32}$$

$$u_n = P_n P_n^T S^T \left(SP_n P_n^T S^T\right)^{-1} (P_c - SQ^\dagger N_c) \tag{33}$$

$$u_n = P_n S^T \left(SP_n S^T\right)^{-1} (P_c - SQ^\dagger N_c) \tag{34}$$

$$u = Q^\dagger N_c + P_n S^T \left(SP_n S^T\right)^{-1} (P_c - SQ^\dagger N_c) \tag{35}$$

References

[1]Schaub, H., Vadali, S. R., and Junkins, J. L., "Feedback Control Law for Variable Speed Control Moment Gyros," *Proceedings of the AAS Spaceflight Mechanics Conference*, Monterey, CA, February 1998, pp. 581–600, paper No. 98-140.

[2]Fausz, J. and Richie, D., "Flywheel Simultaneous Attitude Control and Energy Storage using VSCMGs," *IEEE International Conference on Control Applications*, September 25-27 2000, pp. 991–995, Ancorage, AK.

[3]Richie, D., Tsiotras, P., and Fausz, J., "Simultaneous Attitude Control and Energy Storage using VSCMGs:Theory and Simulation," *Proceedings of the American Control Conference*, June 25-27 2001, pp. 3973–3979, Arlington,VA.

[4]Yoon, H. and Tsiotras, P., "Spacecraft Adaptive Attitude and Power Tracking with Variable Speed Control Moment Gyroscopes," *AIAA Journal of Guidance, Control, and Dynamics*, Vol. 25, No. 6, 2002, pp. 1081–1090.

[5]Yoon, H. and Tsiotras, P., "Singularity Analysis of Variable Speed Control Moment Gyros," *AIAA Journal of Guidance, Control, and Dynamics*, Vol. 27, No. 3, 2004, pp. 374–386.

[6]Wie, B., *Space Vehicle Dynamics and Control*, American Institute of Aeronautics and Astronautics, Inc., Reston, VA, 1998, AIAA Education series.

[7]Schaub, H. and Junkins, J. L., "Singularity Avoidance Using Null Motion and Variable-Speed Control Moment Gyros," *AIAA Journal of Guidance, Control, and Dynamics*, Vol. 23, No. 1, 2000, pp. 11–16.

[8]Wie, B., "New Singularity Escape and Avoidance Steering Logic for Control Moment Gyro Systems," *Proceedings of the AIAA Guidance, Navigation, and Control Conference*, Austin, TX, August 2003.

[9]Bedrossian, N., Paradiso, J., Bergmann, E., and Rowell, D., "Steering Law Design for Redundant Single Gimbal Control Moment Gyroscopes," *AIAA Journal of Guidance, Control, and Dynamics*, Vol. 13, No. 6, 1990, pp. 1083–1089.

[10]Vadali, S., Oh, H., and Walker, S., "Preferred Gimbal Angles for Single Gimbal Control Moment Gyros," *AIAA Journal of Guidance, Control, and Dynamics*, Vol. 13, No. 6, 1989, pp. 1090–1095.

[11]Wie, B., Heiberg, C., and Bailey, D., "Singularity Robust Steering Logic for Redundant Single-Gimbal Control Moment Gyros," *AIAA Journal of Guidance, Control, and Dynamics*, Vol. 24, No. 5, 2001, pp. 865–872.

List of Tables

Table 1:	Simulation Parameters
Symbol	Value
N_{vc}	4
θ, deg	54.75
$\omega(0)$, rad/s	[0 0 0]
$\beta(0)$	[-0.5 0.5 -0.5 0.5]
$\delta(0)$, rad	$[\frac{\pi}{4}\ -\frac{\pi}{4}\ -\frac{\pi}{4}\ \frac{\pi}{4}\ ]$
$\dot{\delta}(0)$, rad/s	[0 0 0 0]
$\Omega(0)$, rpm	[20000 17500 15000 13000]
I_{Wj}, kgm^2	diag{0.70, 0.40, 0.40}
I_{Gj}, kgm^2	diag{0.10 0.10 ,0.10}
I_{sc}, kgm^2	$\begin{bmatrix} 15053 & 3000 & -1000 \\ 3000 & 6510 & 2000 \\ -1000 & 2000 & 11122 \end{bmatrix}$
G	$\begin{bmatrix} 1 & 0.01 & 0.02 \\ 0.01 & 1 & 0.01 \\ 0.02 & 0.01 & 1 \end{bmatrix}$
K,k	diag{0.1, 0.1, 0.1},0.01
μ,μ_2, α, $W_{2_{j_0}}$,$W_{g_{j_0}}$	1, 1000, 10, 0.0001, 1e-4

Table 2: Parametric Comparison of Maximum Attitude Error, Momentum Wheel Torque, Wheel Speed, Average Wheel Speed, and Wheel Speed Difference for a Simultaneous, $5000\,s$ Attitude Plus Power Tracking Maneuver

	Case I				Case II			
$q^T(\beta)\beta_r$, max att error, $X10^{-4}$	3.3015	3.1430	4.4373	4.9126	804.00	192.00	592.00	182.20
CMG #	1	2	3	4	1	2	3	4
$N_{s_{max}}$,Nm	4.1246	2.2569	5.1089	1.6047	0.8587	1.0263	0.7332	0.7715
Ω_{max},10^4 RPM	2.2229	1.9452	2.7262	1.7813	2.2232	1.9467	1.6688	
Ω_{nom},10^4 RPM	1.8201				1.8209			
$\%\,\Omega$	118.86	184.62	254.40	76.699	25.770	11.989	8.3969	23.982

	Case III			
$q^T(\beta)\beta_r$, max att error, $X10^{-4}$	5.6532	3.9822	4.4211	7.5604
CMG #	1	2	3	4
$N_{s_{max}}$,Nm	0.8647	0.7569	0.6486	0.5618
Ω_{max},10^4 RPM	2.2225	1.9456	1.6678	1.4446
Ω_{nom},10^4 RPM	1.8201			
$\%\,\Omega$	25.768	11.983	8.4021	21.663

	Case IV				Case V			
$q^T(\beta)\beta_r$, max att error, $X10^{-4}$	3.5566	3.2771	4.9330	4.6487	3.7380	4.2350	5.1530	4.4840
CMG #	1	2	3	4	1	2	3	4
$N_{s_{max}}$, Nm	0.8640	0.7560	0.6480	0.5616	0.8574	0.7525	0.6427	0.5575
Ω_{max},10^4 RPM	2.2230	1.9451	1.6672	1.4449	2.2234	1.9452	1.6671	1.4446
Ω_{nom},10^4 RPM	1.8201				1.8201			
$\%\,\Omega$	25.768	11.983	8.397	20.622	26.212	7.820	11.295	24.304

List of Figures
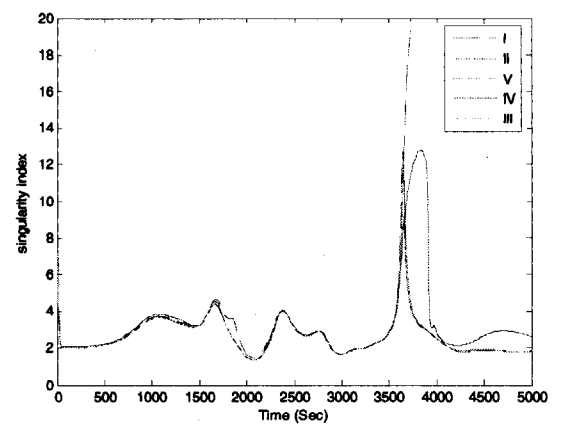
a) Attitude Tracking for Cases I, III, IV, V
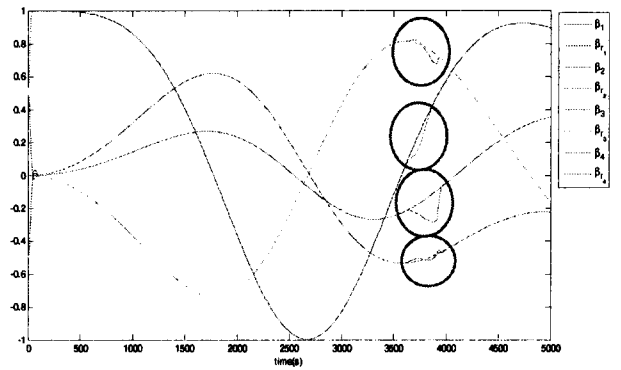
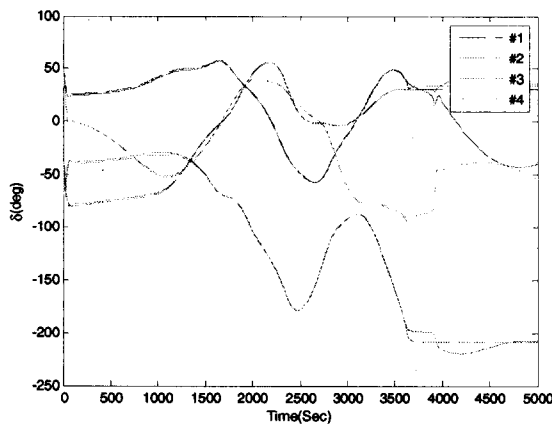
b) Attitude Tracking for Case II
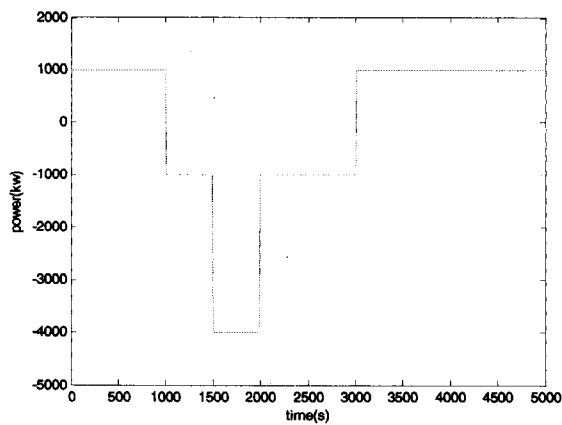
c) Reference and Actual Power Profile for Cases I, III, IV, V
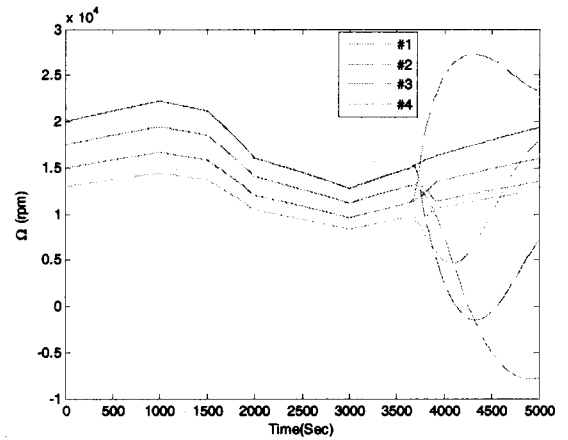

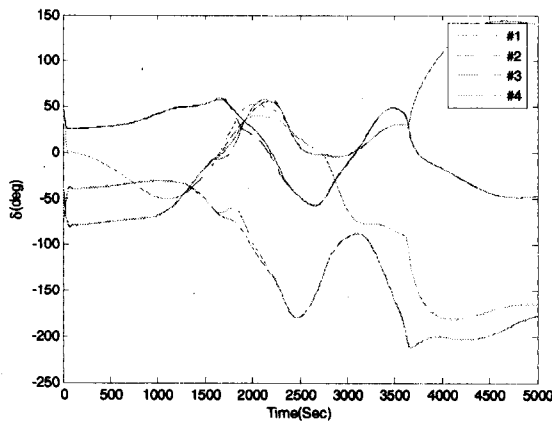**d)** Singularity Condition for Case I-V

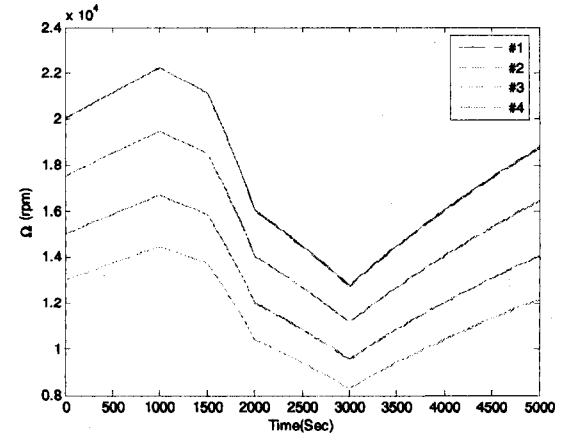**Figure 1:   Attitude, Power Tracking, and Singularity Condition**

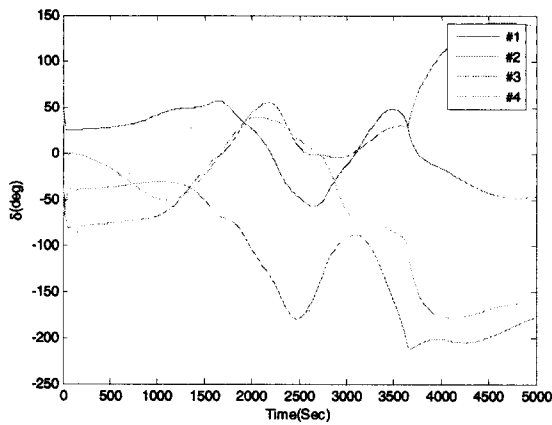**a)** Case I (Baseline) and Case II (GSR) Gimbal Angles

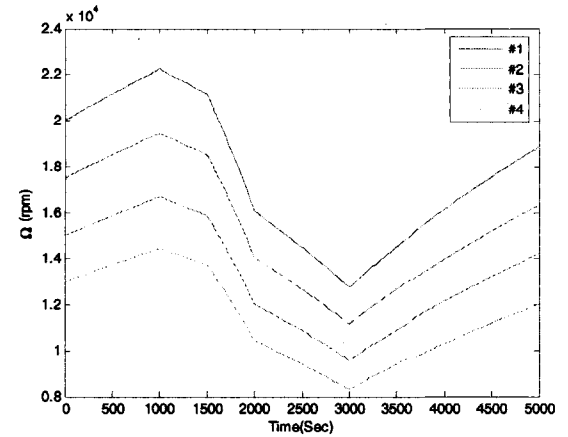**b)** Case I (Baseline) and Case II (GSR) Wheel Speeds

c) Case IV (Schaub) and Case V (Yoon) Gimbal Angles

d) Case IV (Schaub) and Case V (Yoon) Wheel Speeds

e) Case III (Extended GSR) Gimbal Angles

f) Case III (Extended GSR) Wheel Speeds

Figure 2:   Actuator States Comparison